Effects of pinholes on zerooffset of single-axis normal-tracking measurement system

LI Huai-lu[1], WANG Zhong[1], KANG Yan-hui[2], FU Lu-hua[1]

(1. *State Key Laboratory of Precision Measuring Technology and Instrument, Tianjin University, Tianjin 300072, China*; 2. *Division of Metrology in Length and Precision Engineering, National Institute of Metrology, Beijing 100029, China*)

Abstract: A single-axis normal-tracking measurement system is proposed, which can solve the problem of measuring large curved surface. According to Collins formula, the tilt dependent error of the measurement system is studied, which uses Gaussian beam as the light source. By theoretical analysis and numerical simulation, the influence of the error is presented. The results show that there is the difference between point source and Gaussian beam for differential confocal microscopy. The optimal diameter of pinhole can be determined by the mathematical model and the actual parameters of the measurement system. The optimal pinhole diameter of this measurement system is 20 to 35 μm for 633 nm wavelength light source.

Key words: differential confocal microscopy; Gaussian beam; Collins formula; pinhole optimum

CLD number: TP391.4 **Document code**: A

Article ID: 1674-8042(2016)04-0336-06 **doi**: 10.3969/j.issn.1674-8042.2016.04.005

0 Introduction

Confocal microscope is developing rapidly for its high axial and lateral resolution, and it is widely used in many fields such as microelectronics, semiconductor industry, biomedical engineering[1-3]. A number of commercial products based on different confocal principles have been produced in the world, and the studies of confocal microscope are well underway.

WEI Tong-da achieved results about the effects of polarization state and effective numerical aperture on the resolution of confocal total internal reflection microscope in 2014[4]. In 2014, LIU Da-li studied the method and technology to research the real-time laser differential microscope without sample reflectivity[5].

Most of the existing systems are only used for small-angle measurement, and they can not work on the measurement of large curved surface because of the limit of light receiving angle. So a new type of single-axis normal-tracking measurement system is proposed. Single-axis normal-tracking measurement system provides a way to get the axial position based on the method of differential confocal microscope using monochrometic light and laser interference. In order to reduce the disadvantages of the traditional confocal measurements in the large curved surface measurements, position sensitive detectors (PSDs) are added to keep the measurement optical axis be perpendicular to the measurement surface.

The influence of measurement angle in differential confocal microscopy was studied several years ago. ZHANG Jian-huan proved that when the tilt angle of the measurement surface was larger under the point light, the resolution was lower, while the zero position was unchanged. However, the large tilt angle reduces the intensity of light of the pinhole which increases the light intensity measurement error, while increases the accuracy error of measurement for large

Received date: 2016-11-01

Foundation items: Quantity Dissemination and Quality Safety Project of AQSIQ (No. ALC1501); National Key Scientific Instrument and Equipment Development Projects, China (No. 2013YQ170539)

Corresponding author: KANG Yan-hui (kangyh@nim.ac.cn)

curvature[6-7].

However, non-point source is used more frequently than point light source in the actual experiments, such as semiconductor laser, He-Ne laser. Just like Gaussian beam, it has many differences with point light sources as the light sources for the systems. The studies of the systems like single-axis normal-tracking measurement system which uses Gaussian beams as their light sources are not common. In this paper, the model of some important parameters about single-axis normal-tracking measurement system based on Gaussian beam optical field distribution and Collins formula is deduced. The results show that zero error exists in the differential confocal microscopy when the Gaussian beam is used as the light source, which is different from point light source. The optimal diameter of pinhole can be achieved by the model, which provided an important reference to similar researches.

1 Principle of single-axis normal-tracking measurement system

The optical principle is shown in Fig. 1. Linear polarized Gaussian beam (1) is divided into two beams by a nonpolarizing beam splitter (NPBS) (4) after passing through the polarization beam splitter (PBS) (2) and the quarter-wave plate (3). One is reflectedto the surface of a position sensitive detector (PSD) (5). The other one is reflected by the object under test (7) after passing through the micro objective (6), and then passes through them again.

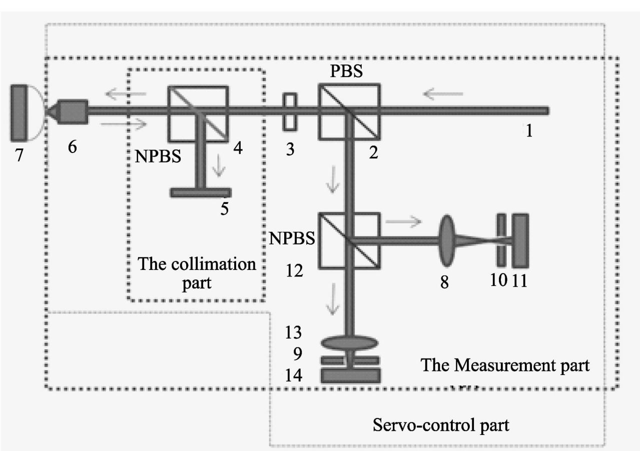

Fig. 1 Optical principle

The photodetectors (11, 14) receive the signals through the pinholes (9,10) after the beam reflected by the PBS (2), divided by NPBS (12), and collected by the focusing lens (8,13). The positions of two pinholes are different (front and back to the focal point). The relative height can be calculated by the differential signal based on the differential confocal theory. The angle between optical axis and the object under test can be real-time measured by the offset distance on the PSD. Then the verticality is controlled by the servo device. The surface profile can be measured finally.

2 Key influence factors

In the ideal case, the optic axis is constantly perpendicular to the surface under test. However, due to several influential factors, the above conditions can not be satisfied, which bring huge impacts on the system.

Because of the variations in different systems designs, the reasons of misalignment are different. The following is a list of the main reasons which will appear in each of the systems.

2.1 Position precision of PSD

For simplicity, the two-dimensional case is only considered, and the high-dimensional cases can be derived by using the same method. As shown in Fig. 2, the position error of the PSD, δ, causes the angle error, θ.

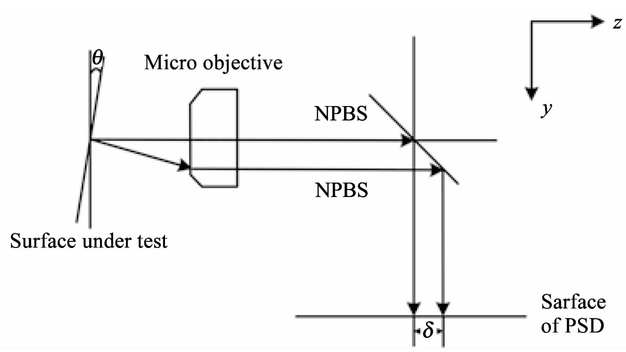

Fig. 2 Position precision of PSD may lead to calculation deviation between optic axis and surface under test

If the focal length of the micro objective is f_1, then

$$\theta = \frac{1}{2}\arctan\left(\frac{\delta}{f_1}\right). \tag{1}$$

2.2 Positioning error of servo motors

In different systems, the algorithms are different, and the types of selected motors are different, which may be linear motors or rotary motors, whichever will lead to the deviation of axial position.

The two-dimensional case is also only considered, as shown in Fig. 3. The linear motors of Y and Z axes are used to reposition the probe and the rotary motor is used to make the optic axis perpendicular to the surfaceunder test. However, the error of the rotary motor, ε_{yz}, will lead to an angle error, α.

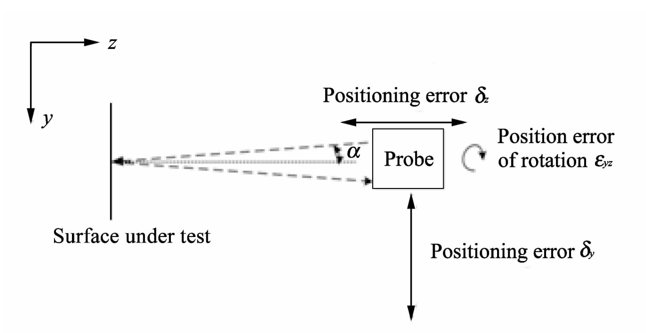

Fig. 3 Angle error caused by position error of servo motors

2.3 Angular deviation between optic axis of the micro objective and normal of the surface under test

Because of the installation error, the optic axis ofthe micro objective is not completely perpendicular to the surface under test, so the reflected light will not transmit along the original way. Beyond these points, there are also other more or less factors, which will lead to an angular deviation between the reflected measuring light and the surface under test. The facts will also make the actual results different from the theoretical results. So it is necessary to study the influence of tilt the measurement system, which can be attributed to that the surface is inclined relative to the optic axis.

3 Theoretical analysis and numerical simulation

Optical field distribution of Gaussian incident beam can be expressed as Eq. (2)[8],

$$E(x,y,z)=\left[\frac{A_0}{\omega(z)}\exp\left(-\frac{x^2+y^2}{\omega^2(z)}\right)\right]\exp\left\{-\mathrm{i}k\left[z+\frac{x^2+y^2}{2R(z)}\right]+\mathrm{i}\varphi(z)\right\}, \tag{2}$$

where
$$\omega(z)=\omega_0\sqrt{1+\left(\frac{\lambda z}{\pi\omega_0^2}\right)^2},$$
$$R(z)=z\left[1+\left(\frac{\pi\omega_0^2}{\lambda z}\right)^2\right],$$
$$\varphi(z)=\arctan\left(\frac{\lambda z}{\pi\omega_0^2}\right).$$

When the Gaussian beam passes through a micro objective, its parameters will be changed, as shown in Fig. 4.

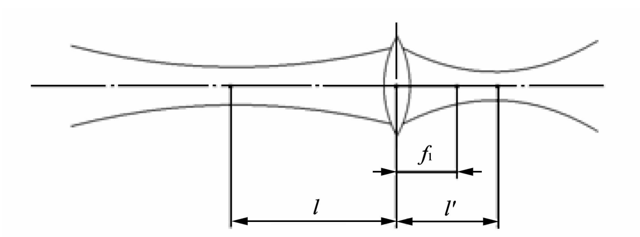

Fig. 4 Parameters of the beam are changed after passing through a micro objective

The new waist, ω_0', and the distance between the new waist and the focus point of the micro objective, $l'-f_1$, can be expressed as[9]

$$\omega_0'=\sqrt{\frac{\omega^2}{(1-1/f_1)^2+(z_r/f_1)^2}}, \tag{3}$$

$$l'-f_1=\frac{l-f_1}{(1-l/f_1)^2+(z_r/f_1)^2}, \tag{4}$$

where ω is the Gaussian incident beam's waist, l is the distance between the Gaussian incident beam' waist and the focus point, and f_1 is the focal length of the micro objective.

When the coordinate system, XYZ, rotates θ around the axis X, the point (x,y,z) will be new coordinates (x', y', z'). The transformed rotational matrix can be expressed as[10]

$$\begin{bmatrix}x'\\y'\\z'\end{bmatrix}=\begin{bmatrix}1 & 0 & 0\\0 & \cos\theta & \sin\theta\\0 & -\sin\theta & \cos\theta\end{bmatrix}\begin{bmatrix}x\\y\\z\end{bmatrix}. \tag{5}$$

Optical field after redefining the coordinate system is

$$E'(x,y,z)=\frac{A_0}{\omega'(y\sin\theta+z\cos\theta-l'+f_1)}\exp\left[-\frac{x^2+(y\cos\theta-z\sin\theta)^2}{\omega'^2(y\sin\theta+z\cos\theta)}\right]\cdot$$

$$\exp\left\{-\mathrm{i}k\left[(y\sin\theta+z\cos\theta-l'+f_1)+\frac{x^2+(y\cos\theta-z\sin\theta)^2}{2R(y\sin\theta+z\cos\theta-l'+f_1)}\right]+\mathrm{i}\varphi(y\sin\theta+z\cos\theta-l'+f_1)\right\}. \quad (6)$$

When $z=-f_1$, the optical field is

$$U_1(x,y)=\frac{A_0}{\omega'(y\sin\theta+f_1\cos\theta-l'+f_1)}\exp\left[-\frac{x^2+(y\cos\theta-f_1\sin\theta)^2}{\omega'^2(y\sin\theta+f_1\cos\theta)}\right]\cdot$$

$$\exp\left\{-\mathrm{i}k\left[(y\sin\theta+f_1\cos\theta-l'+f_1)+\frac{x^2+(y\cos\theta-f_1\sin\theta)^2}{2R(y\sin\theta+f_1\cos\theta-l'+f_1)}\right]+\mathrm{i}\varphi(y\sin\theta+f_1\cos\theta-l'+f_1)\right\}. \quad (7)$$

The expression of paraxial rays is given by

$$U_1(x,y)=\frac{A_0}{\omega'(y\theta+2f_1-l')}\exp\left[-\frac{x^2+(y-f_1\theta)^2}{\omega'^2(y\theta+f_1)}\right]\cdot$$

$$\exp\left\{-\mathrm{i}k\left[(y\theta+2f_1-l_1')+\frac{x^2+(y-f_1\theta)^2}{2R(y\theta+2f_1-l')}\right]+\mathrm{i}\varphi(y\theta+2f_1-l')\right\}. \quad (8)$$

The Collins formula[11] is

$$U_2(x_2,y_2)=\left(-\frac{\mathrm{i}}{\lambda B}\right)\iint U_1(x_1,y_1)\exp[\mathrm{i}kw(x_1,y_1,x_2,y_2)]\mathrm{d}x_1\mathrm{d}y_1, \quad (9)$$

where $w(x_1,y_1,x_2,y_2)=L_0+\frac{1}{2B}[A(x_1^2+y_1^2)-2(x_1x_2+y_1y_2)+D(x_2^2+y_2^2)]$; $U_1(x_1, y_1)$ and $U_2(x_2, y_2)$ are the field amplitudes of incident plane and the exit plane; k is the wave vector; L_0 is the optical path along the axis between incident plane and the exit plane, A, B, C and D are the parameters of optical transformation matrix. The $ABCD$ matrix from the focus point to the focusing lens is

$$\begin{bmatrix}A & B\\ C & D\end{bmatrix}=\begin{bmatrix}1 & 0\\ -\frac{1}{f_2} & 1\end{bmatrix}\begin{bmatrix}1 & L\\ 0 & 1\end{bmatrix}\begin{bmatrix}1 & 0\\ -\frac{1}{f_1} & 1\end{bmatrix}\begin{bmatrix}1 & f_1\\ 0 & 1\end{bmatrix}=\begin{bmatrix}1-\frac{L}{f_1} & f_1\\ \frac{L}{f_1f_2}-\frac{1}{f_1}-\frac{1}{f_2} & -\frac{f_1}{f_2}\end{bmatrix}. \quad (10)$$

So the optical field behind the focusing lens according to the Collins formula is

$$U_2(x_2,y_2)=\frac{\mathrm{e}^{\mathrm{i}\left(kL_1-\frac{\pi}{2}\right)}}{\lambda f_1}\iint U_1(x_1,y_1)\mathrm{e}^{\frac{\mathrm{i}k}{2f_1}\left[\left(1-\frac{L}{f_1}\right)(x_1^2+y_1^2)-2(x_1x_2+y_1y_2)+\left(-\frac{f_1}{f_2}\right)(x_2^2+y_2^2)\right]}\mathrm{d}x_1\mathrm{d}y_1. \quad (11)$$

Two pinholes are set on different sides of the focusing lens. If the distance between the pinhole and the focusing lens is u_{ph}, the $ABCD$ matrices are

$$\boldsymbol{M}_1=\begin{bmatrix}1 & f_2-u_{\mathrm{ph}}\\ 0 & 1\end{bmatrix}, \quad (12)$$

$$\boldsymbol{M}_2=\begin{bmatrix}1 & f_2+u_{\mathrm{ph}}\\ 0 & 1\end{bmatrix}. \quad (13)$$

So the optical fields behind the pinholes are

$$U_3(x_3,y_3)=\frac{\mathrm{e}^{\mathrm{i}\left[k(f_2-u_{\mathrm{ph}})-\frac{\pi}{2}\right]}}{\lambda(f_2-u_{\mathrm{ph}})}\iint U_2(x_2,y_2)\cdot \mathrm{e}^{\frac{\mathrm{i}k}{2(f_2-u_{\mathrm{ph}})}[(x_2-x_3)^2+(y_2-y_3)^2]}\mathrm{d}x_2\mathrm{d}y_2, \quad (14)$$

$$U_4(x_4,y_4)=\frac{\mathrm{e}^{\mathrm{i}\left[k(f_2-u_{\mathrm{ph}})-\frac{\pi}{2}\right]}}{\lambda(f_2+u_{\mathrm{ph}})}\iint U_2(x_2,y_2)\cdot \mathrm{e}^{\frac{\mathrm{i}k}{2(f_2+u_{\mathrm{ph}})}[(x_2-x_4)^2+(y_2-y_4)^2]}\mathrm{d}x_2\mathrm{d}y_2. \quad (15)$$

The function of a pinhole whose radius is r can be expressed as

$$P(x,y)=\begin{cases}1 & x^2+y^2\leqslant r^2,\\ 0 & x^2+y^2>r^2.\end{cases} \tag{16}$$

Therefore, the tilt dependent error (*TDE*) can be calculated by

$$TDE(r,u_{ph})=\frac{\dfrac{\iint U_3(x_3,y_3)P(x_3,y_3)\mathrm{d}x_3\mathrm{d}y_3}{\iint U_3(x_3,y_3)\mathrm{d}x_3\mathrm{d}y_3}-\dfrac{\iint U_3(x_4,y_4)P(x_4,y_4)\mathrm{d}x_4\mathrm{d}y_4}{\iint U_3(x_4,y_4)\mathrm{d}x_4\mathrm{d}y_4}}{\dfrac{\iint U_3(x_3,y_3)P(x_3,y_3)\mathrm{d}x_3\mathrm{d}y_3}{\iint U_3(x_3,y_3)\mathrm{d}x_3\mathrm{d}y_3}+\dfrac{\iint U_3(x_4,y_4)P(x_4,y_4)\mathrm{d}x_4\mathrm{d}y_4}{\iint U_3(x_4,y_4)\mathrm{d}x_4\mathrm{d}y_4}}. \tag{17}$$

It should be noted that axial displacement and radial displacement are not normalized, because the tilt makes them interact each other.

According to the actual system parameters and the above-mentioned expressions, the *TDE* is shown in Fig. 5.

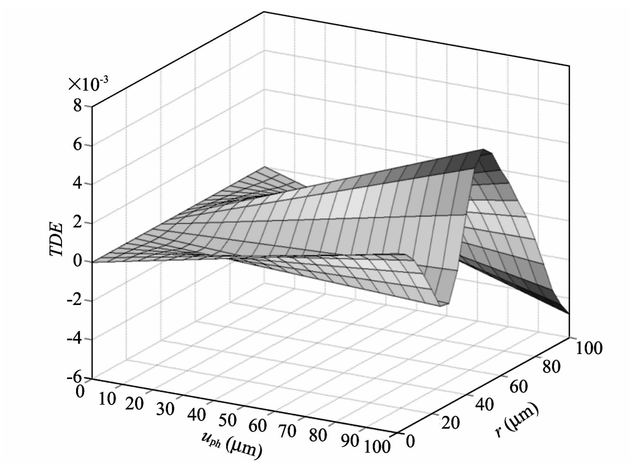

Fig. 5 ***TDE*(*r*, u_{ph})**

Fig. 5 shows the relation between r, u_{ph} and *TDE*. For different u_{ph}, the curve between *TDE* and r are shown in Fig. 6.

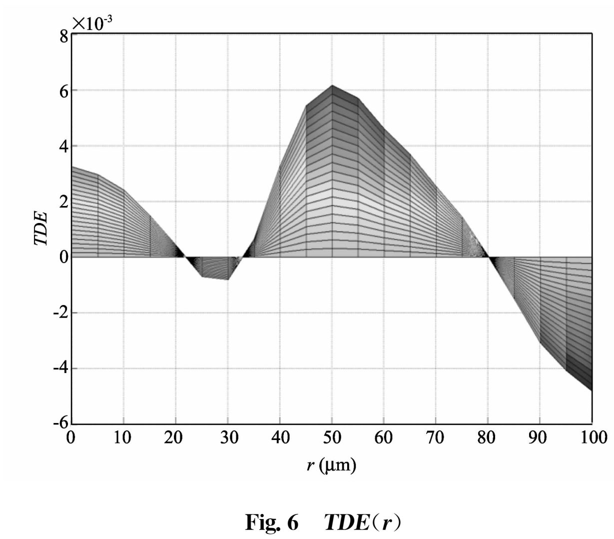

Fig. 6 ***TDE*(*r*)**

As shown in Fig. 5, *TDE* and u_{ph} is approximately linearity, and the optimal value of u_{ph} can not be obtained. So the optimal value of u_{ph} needs to be calculated by other methods, and the optimal value is the value which matches the highest sensitivity of the Gaussian beam. The optimal value of u_{ph} can be calculated by taking the derivative of the cross-sectional areas formula of the Gaussian beam, and it is the Rayleigh range. From the Fig. 6, the radius of the pinhole has the optimal value, which is about 20 to 35 μm. However, the figures above are based on the actual parameters, so the optimal value inpractical application should be calculated by above equations.

4 Conclusion

A novel single-axis normal-tracking measurement system is introduced. Based on the Collins formula and optical field distribution formula of Gaussian beam, the theoretical model of tilt dependent error about pinhole radius and axial offset is derived. Then the calculation is got by numerical analysis about the theoretical model. The calculation shows that there is the difference between point light source and Gaussian beam in differential confocal microscopy just like single-axis normal-tracking measurement system. The zero position will offset in the Gaussian beam optical system. According to the model above and the actual parameters, the optimal value inpractice can be calculated.

References

[1] HE Yan-wen, CHENG Yi, TANG Zhi-lie. Imaging investigation of polarization control microscope based on stokes parameters of weak anisotropic substances. Acta Laser Biology Sinica, 2016, 44(1): 21-26.

[2] ZHU Zu-song, ZHANG Jie, YI Ming-fang, et al. Prepara-

tion of the high-quality and stable microcrystalline silicon films. Journal of Sichuan University(Natural Science Edition), 2016, 53(1): 157-162.

[3] MA Yu-fan, SHENG Lei-mei. Study on the preparation and performance of multi-walled carbon nanotubes as conductive agent of lithium ion battery. New Chemical Materials, 2016, 44(1): 43-45.

[4] WEI Tong-da, ZHANG Yun-hai, XIAO Yun, et al. Effects of polarization state and effective numerical aperture on the resolution in confocal total internal reflection microscopy. Laser & Optoelectronics Progress, 2014, 51(1): 315-321.

[5] Qiu L, Liu D, Zhao W, et al. Real-time laser differential confocal microscopy without sample reflectivity effects. Optics express, 2014, 22(18): 21626-21640.

[6] ZHANG Jian-huan, TAN Jiu-bin. Theoretical analysis of surface slope measurement with a confocal microscope. Journal of Optoelectronics Laser, 2002, 13(12): 1272-1275.

[7] HOU Mao-sheng. Study on key techniques of profile measurement for large aperture optical aspherics, 2015.

[8] GAO Yu-han. Research of Gaussian beam shaping. Changchun: Changchun University of Science and Technology, 2012.

[9] GE Hua, YANG Kun-tao. The research of conversion of off-axis Gaussian beam passing through optical system. Laser & Infrared, 2003, 33(1): 68-70.

[10] ZHU Lei-ming, WU Xiao-ping, LI Jian-wei, et al. The euler's rotation and dynamic equation of rectangular coordinate system. Hydrographic Surveying and Charting, 2010, 30(3): 9-12.

[11] DING Gui-lin. Collins formula and its applications in optics. Chinese Journal Of Quantum Electronics, 1990, 7(3): 221-227.

针孔对单轴法线跟踪式测量系统零位测量的影响

李怀禄[1]，王　仲[1]，康岩辉[2]，付鲁华[1]

(1. 天津大学 精密测试技术与仪器国家重点实验室，天津 300072；
2. 中国计量科学研究院 长度计量科学与精密机械测量技术研究所，北京 100029)

摘　要： 针对大曲率表面面形测量问题，提出一种单轴法线跟踪式测量方法。通过运用 Collins 公式，研究了倾斜角度对基于高斯光束测量系统的影响；通过理论分析和数值模拟，证明了在待测面倾斜的情况下，高斯光束与点光源作用下差动共焦系统的零位位置有明显不同；推导出高斯光束测量系统中针孔最佳尺寸和实际系统参数的关系，指出实验中波长为 633 nm 测量系统的针孔最佳直径在 20 μm 到 35 μm 之间。

关键词： 差动共焦；高斯光束；Collins 公式；针孔最佳尺寸

引用格式： LI Huai-lu, WANG Zhong, KANG Yan-hui, et al. Effects of pinholes on zerooffset of single-axis normal-tracking measurement system. Journal of Measurement Science and Instrumentation, 2016, 7(4): 336-341. [doi: 10.3969/j.issn.1674-8042.2016.04.005]